ISBN: 978-3-95450-208-0 doi:10.18429/JACoW-IPAC2019-TUPRB090

PRELIMINARY CONSIDERATIONS OF ATOMIC INNER-SHELL X-RAY LASER FOR SELF-SEEDING AT LCLS-II

A. Halavanau[1], A. Benediktovitch[2], N. Rohringer[2], J. Wu[1], C. Pellegrini[1]
[1] SLAC National Accelerator Laboratory, Stanford University, Menlo Park CA 94025, USA
[2] Center for Free Electron Laser Science, DESY, Hamburg, Germany

Abstract

The atomic inner-shell X-ray lasing, induced by the irradiation of focused XFEL SASE pulses, was demonstrated in gases, liquid jets and solids. In this proceeding, we discuss the possible use of this concept in self-seeding scheme at LCLS-II. We provide a preliminary study of different lasing media and corresponding SASE XFEL parameters. For the case of noble gas inner-shell X-ray laser, we study the requirements for gas pressure and XFEL pulse focusing. Finally, we discuss possible designs of this system and its advantages in LCLS-II operations.

OVERVIEW OF ATOMIC INNER-SHELL X-RAY LASING

Atomic inner-shell X-ray laser (XRL) concept has been theoretized in the 60s and experimentally verified in the recent experiments at LCLS facility and worldwide. The most recent experimental realizations of atomic XRL include lasing with Ne gas [1, 2], Mn(II) and Mn(VII) complexes in solution [3], Cu metallic foil [4].

The principle of the atomic XRL is attributed to fast photoionization of the inner-most atomic levels, yielding population inversion. The spontaneous fluorescent radiation in such medium undergoes amplification, and, if the amount of inverted atoms is large enough, superfluorescence can take place. In this case the stimulated fluorescence becomes the dominant process of deexcitation of atoms, and the stored energy of atomic excitation is released in the form of short bursts in the forward direction. This phenomenon is known in optical domain [5], however in X-ray domain specifics of pumping and competing de-excitation processes should be considered – resulting in need for dedicated approaches suitable in the X-ray domain. The simplest approach based on rate equations for atomic state occupations and radiation flux [6] can provide estimates on the intensity gain. A more detailed description including spectral properties as well as strong non-linear behavior (like Rabi oscillations) can be obtained based on semi-classical Maxwell-Bloch approach. However, the semi-classical Maxwell-Bloch equations do not describe the quantum properties of the electromagnetic field that manifest themselves as spontaneous emission and seeds the intensity growth. In order to model them, a semi-phenomenological noise terms were introduced in the equations describing the atomic polarization [7, 8]. However, this approach is known to describe incorrectly the initial stage of the amplification process [9]. Recently, a unified description of both spontaneous and stimulated radiation processes was proposed in [10], the description is based on equations for two-point correlation functions.

PROPOSED EXPERIMENTAL SETUP

A common requirement for the self-seeding in XFELs is the narrow bandwidth of the seeding radiation. It can be achieved in several ways, e.g. including, diffraction gratings, transmissive and reflective crystals inserted in the SASE pulse optical path. Due to selective Bragg diffraction process, the resulting bandwidth is significantly reduced compared to the original SASE pulse. The typical bandwidth in current soft X-ray (SXR) self-seeding grating systems is 5×10^{-4}. Atomic XRL, due to the discrete quantum nature of the atomic levels, is an excellent candidate for X-ray monochromator. It is, however, not tunable on the contrary to a reflective/transmissive crystal, and thus such self-seeding method can be considered as complimentary to the existing ones.

Our proposed experimental setup shown in Fig. 1 consists of a short SASE undulator section, an electron beam chicane with a gas cell mounted in the middle, and the tapered amplifier undulator section downstream of the chicane. It is identical to the existing SXR/HXR self-seeding setup with the crystal being replaced with a gas cell. To assess the performance of a gas cell, we considered LCLS-II SXR/HXR undulators beamline with the existing self-seeding setup replaced with an atomic XRL. We first note that a similar setup has been recently investigated in [11]. In this proceeding, we restrict our study to the regular two stage self-seeding with no X-ray focusing into the gas-cell. The formalism developed in [10] allows for the XRL performance calculation, therefore one can estimate the optimum macroscopic gas parameters, such as pressure, temperature and resulting gas cell length for a maximum photon yield. One possible setup, the noble gas is constantly pumped through a rectangular nozzle with small apertures on the sides for incoming/outgoing X-rays. The gas is recirculated to maintain constant temperature and pressure, and corresponding XFEL pulse parameters are ganged in Tab. 2. In the simulations we consider a flat rectangular sheet of gas of the width z traversing through the vacuum chamber under constant pressure.

Self-Seeding with a Noble Gas

Naturally, the most convenient element for atomic XRL application in self-seeding is a noble gas. Here we investigate potential noble gas choices for SXR/HXR self-seeding assuming XRL operates on inner-most K-shell levels only.

ISBN: 978-3-95450-208-0 doi:10.18429/JACoW-IPAC2019-TUPRB090

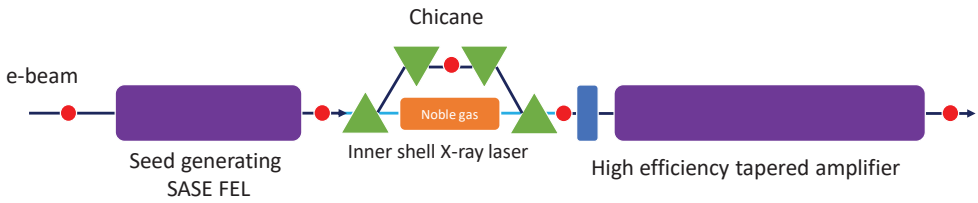

Figure 1: Atomic gas XRL self-seeding schematics.

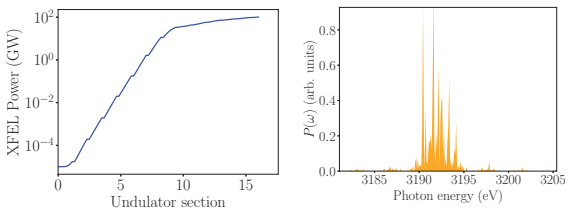

Figure 2: Nominal LCLS-II HXR SASE performance at 3 keV. XFEL power as a function of undulator section (left) and SASE spectral content (right).

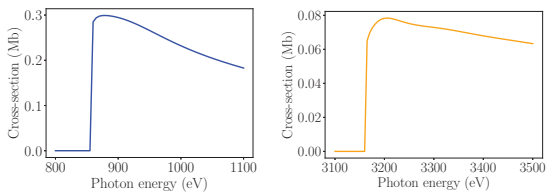

Figure 3: Photoionization cross-sections of the inner-most atomic level of Neon (left) and Argon (right) as a function of XFEL pulse energy. The values are calculated in XATOM package. 1 Mbarn is 10^{-4} nm^2.

For SXR self-seeding one can use Neon gas, similarly to the seminal experiment at LCLS [1]. We also refer the reader to [1] for the experimental demonstration of bandwidth reduction.

For tender X-rays (3 keV) the next noble gas candidate is Argon. With the increase of atomic number Z, the Auger decay time of K-shell levels becomes smaller as well as the photoionization cross-section, which results in higher pump values needed for XRL process. Thus, photon energies for HXR self-seeding are harder to access with the inner-shell XRL in noble gases. Here we will consider the application of this concept to soft and tender X-rays only.

Other Choices of Lasing Medium

In order to further allure possible XRL-seeded XFEL applications, we diversify the choices of lasing media with other chemical elements; see Tab. 1. We note, that from practical standpoint every chemical element has to be evaluated for possible chemical interactions with the beampipe walls. However, here we refrain from a specific chamber design considerations and restrict our study to academic interest only. Similarly to [3], elements with $11 < Z < 17$ can be utilized in XRL in the form of laminar liquid jets of chemical solutions. This would allow for discrete tunability of the XRL. In combination with lasing on multiple atomic levels, the degree of tunability is further increased.

Table 1: Inner-most Atomic Levels in the SXR Range of the First Several Elements in the Periodic Table [15]

Z	Element	Kα_2 (eV)	Kα_1 (eV)
10	Ne	848.61	848.61
11	Na	1040.98	1040.98
12	Mg	1253.44	1253.69
13	Al	1486.30	1486.71
14	Si	1739.39	1739.99
15	P	2012.70	2013.69
16	S	2306.70	2307.89
17	Cl	2620.85	2622.44
18	Ar	2955.57	2957.68
19	K	3311.20	3313.95
20	Ca	3688.13	3691.72

FEL NUMERICAL SIMULATIONS

We first focus on the limiting case of 3 keV photons. FEL simulations for LCLS-II HXR undulator have been performed in customary GENESIS code [12]. It was then wrapped in a framework for tapering optimization [13] first introduced in [14].

We considered realistic electron beam parameters (4 kA peak current, 15 fs flat-top current profile with normalized transverse emittance of 0.4μm). Typical XFEL pulse spot-size is assumed to be 12 μm. Gain curve and SASE spectrum is presented in Fig. 2. The atomic XRL is placed in the second self-seeding chicane at U16. We refer the reader to [16] for detailed LCLS-II technical design.

ATOMIC GAS NUMERICAL SIMULATIONS

In this section we present numerical results for the cases of Neon and Argon gas self-seeding. Simulation parameters for Neon and Argon are shown in Tab. 2. The values of Auger times and photoionization cross-sections were calculated using XATOM package [17, 18]. We used the numerical code that implemented the two-point correlations function approach and was developed for superfluorescence calculations in [10]. The photoionization curves shown in Fig. 3 show typical threshold behavior, meaning that entire SASE

ISBN: 978-3-95450-208-0 doi:10.18429/JACoW-IPAC2019-TUPRB090

Table 2: XRL Simulation Parameters for Neon and Argon Gases

Parameter	Units	Neon	Argon
Pump duration	fs	15	5-10
N photons	$\times 10^{12}$	1-10	1-10
FEL power, max	GW	70	480
FEL power, min	GW	7	48
X-ray spotsize	μm	1-20	1 -20
Pressure	mBar	500	500
Chamber length	mm	15	30
Auger decay	fs	2.4	1.1
Radiation lifetime	fs	160	7.5
Photoionization, σ	$\times 10^{-5}$nm^2	3.0	0.76

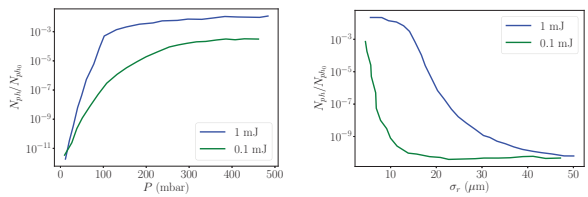

Figure 4: Simulated superfluorescence photon yield in Neon gas for different XFEL pump pulse energies as a function of pressure (left) and XFEL pulse spotsize (right).

pulse with the photon energy above threshold will participate in XRL pumping. We also notice that photoionization cross-section becomes an order of magnitude lower between the cases of Neon and Argon.

Let us first consider the case of Neon gas. As expected, increasing gas chamber pressure helps to significantly increase photon yield; see e.g. Fig. 4. With respect to variation of spotsize of the XFEL pulse, the photon yield efficiency was found to be highly non-linear. At low XFEL intensities a substantial focusing is required in order to go above 10^{-6} efficiency which is associated with the noise level. At high XFEL intensity, however, no focusing is required for the yield efficiency in the order of 10^{-2}.

Thus, in order to reach the required photon intensity, one has to optimize FEL performance in the SASE section for maximum power output. The advantage of atomic XRL self-seeding compared to reflective/transmissive crystal is no power limitation due to thermal damage, therefore, in

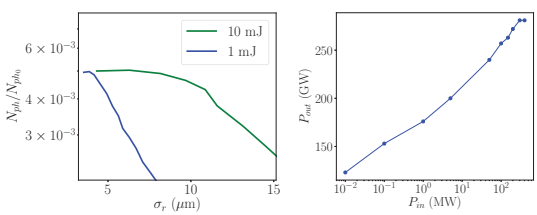

Figure 5: Simulated superfluorescence photon yield in Argon gas as a function of XFEL pulse spotsize (left). Output XFEL power as a function of seeding power (right).

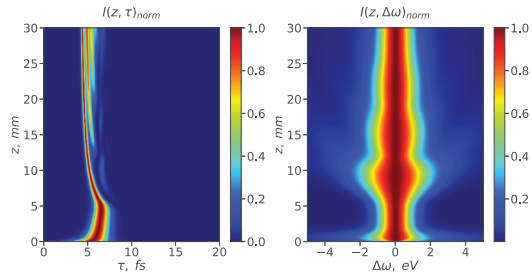

Figure 6: Numerical simulation of superfluorescence in Argon induced by XFEL pulse of 10 mJ. Intensity as a function of z and time τ (left) and resulting bandwidth (right).

principle, Neon gas cell can provide higher output seeding power. It will also withstand LCLS-II SRF high rep-rate SXR pulses. We now move on to the case of Argon gas self-seeding. We first note that due to an order of magnitude lower photoionization cross-section (see Fig. 3), the optimum XFEL intensity is also increased by an order of magnitude; see Fig. 5. XFEL pulse energy of 10 mJ at 3 keV photon energy becomes debatable, thus we consider it as an upper bound case. Similarly, pulse energy of 1 mJ would not provide enough secondary photons without additional focusing to about 7 μm, therefore is considered as a lower bound. Figure 5 (right) illustrates the final FEL power output after strong tapering. For the pulse energies above 1 mJ the conversion efficiency is estimated to be 0.1%. An example calculation of gain and bandwidth evolution with the gas interaction length z is shown in Fig. 6. The value of bandwidth is comparable to the best measured so far in HXRSS setup at LCLS.

SUMMARY

In summary, we evaluated, via numerical calculations, the atomic gas monochromator concept at LCLS-II SXR and HXR beamlines for 0.85 and 3.0 keV respectively. We found, that due to lower photoionization crossection and short Auger decay time of the inner-most Argon atomic level, XRL self-seeding requires significant increase of the SASE power. Alternatively, an X-ray focusing element may be introduced to increase photon irradiation intensity. At soft X-ray photon energy, however, atomic inner-shell Neon XRL conversion efficiency is enough to aid in self-seeding process. Albeit being fixed to a specific wavelength, XRL self-seeding can be extended to the case of multiple electron bunches and XFEL pump-probe schemes [19].

ACKNOWLEDGEMENTS

This work was supported by the U.S. Department of Energy Contract No. DE-AC02-76SF00515. We would like to thank DESY XRAYPAC group for providing us XATOM software. A. H. would like to thank I. Nam (PAL, Korea); A. Marinelli, E. Hemsing, G. Marcus (SLAC) for their interest in the subject and useful discussions.

ISBN: 978-3-95450-208-0 doi:10.18429/JACoW-IPAC2019-TUPRB090

REFERENCES

[1] N. Rohringer, *et al*, *Nature*, 481:488-491, EP, (2012).

[2] C. Weninger, *et al*, *Phys. Rev. Lett.*, 111:233902, (2013).

[3] T. Kroll, *et al*, *Phys. Rev. Lett.*, 120:133203, (2018).

[4] H. Yoneda, *et al*, *Nature*, 524:446–449, 08, (2015).

[5] M. Gross and S. Haroche, *Physics Reports*, 93:5, 301-396, (1982)

[6] N. Rohringer and R. London, *Phys. Rev. A*, 80:013809, (2009).

[7] O. Larroche, D. Ros, A. Klisnick, A. Sureau, C. Möller, and H. Guennou. *Phys. Rev. A*, 62:043815, (2000).

[8] C. Weninger and N. Rohringer. *Phys. Rev. A*, 90:063828, (2014).

[9] Š. Krušič, K. Bučar, A. Mihelič, and M. Žitnik. *Phys. Rev. A*, 98:013416, (2018).

[10] A. Benediktovitch, V. P. Majety, and N. Rohringer. *Phys. Rev. A*, 99:013839, (2019).

[11] H. Zhang, K. Li, J. Yan, H. Deng, and B. Sun. *Phys. Rev. Accel. Beams*, 21:070701, (2018).

[12] S. Reiche. GENESIS 1.3: a fully 3D time-dependent FEL simulation code. *Nuclear Instruments and Methods in Physics Research A*, 429:243–248, (1999).

[13] C. Mayes and A. Halavanau. lume-genesis package. *lume-genesis package,* `https://github.com/slaclab/lume-genesis`.

[14] A. Halavanau, F.-J. Decker, C. Emma, J. Sheppard, and C. Pellegrini. *Journal of Synchrotron Radiation*, 26(3), (2019).

[15] Provided by NIST, https://www.nist.gov, (2019).

[16] H. D. Nuhn, *Report No. SLAC-I060-003-000-07-R000*, (2011).

[17] Z. Jurek, S.-K. Son, B. Ziaja, and R. Santra. *Journal of Applied Crystallography*, 49(3):1048–1056, (2016).

[18] S.-K. Son, L. Young, and R. Santra. *Phys. Rev. A*, 83:033402, (2011).

[19] F.-J. Decker, K. Bane, W. Colocho, A. Lutman, and J. Sheppard. In *Proceedings, 38th International Free Electron Laser Conference, FEL2017*, page TUP023, (2018).